# Multisensory integration enhances audiovisual responses in the Mauthner cell

Santiago Otero-Coronel[1], Thomas Preuss[2] and Violeta Medan[1,3]*

*Abbreviated title:* Multisensory integration in the Mauthner cell

1. Instituto de Fisiología y Biología Molecular y Celular, Consejo Nacional de Investigaciones Científicas y Tecnológicas, Buenos Aires, Argentina (1428).
2. Dept. Psychology, Hunter College, City University of New York, New York, NY, USA (10065).
3. Dept. Fisiología y Biología Molecular y Celular, Facultad de Ciencias Exactas y Naturales, Universidad de Buenos Aires, Buenos Aires, Argentina (1428).

*Corresponding author, e-mail: violetamedan@fbmc.fcen.uba.ar.

Conflict of interest statement: The authors declare no competing financial interests.

ABSTRACT

Multisensory integration combines information from multiple sensory modalities to create a coherent perception of the world. In contexts where sensory information is limited or equivocal, it also allows animals to integrate individually ambiguous stimuli into a clearer or more accurate percept and, thus, react with a more adaptive behavioral response. Although responses to multisensory stimuli have been described at the neuronal and behavioral levels, a causal or direct link between these two is still missing. In this study, we studied the integration of audiovisual inputs in the Mauthner cell, a command neuron necessary and sufficient to trigger a stereotypical escape response in fish. We performed intracellular recordings in adult goldfish while presenting a diverse range of stimuli to determine which stimulus properties affect their integration. Our results show that stimulus modality, intensity, temporal structure, and interstimulus delay affect input summation. Mechanistically, we found that the distinct decay dynamics of feedforward inhibition triggered by auditory and visual stimuli can account for certain aspects of input integration. Altogether, this is a rare example of the characterization of multisensory integration in a cell with clear behavioral relevance, providing both phenomenological and mechanistic insights into how multisensory integration depends on stimulus properties.

## INTRODUCTION

The ability to detect a potential threat and react with an escape behavior is critical for survival. In nature, however, many predators develop strategies such as camouflage or partial hiding to decrease their salience, and sensory stimuli tend to be noisy and ambiguous. Consequently, it is adaptive for animals to have ways to disambiguate the signals from the sensory inflow they receive, especially in contexts where available information is limited.

One strategy for reducing sensory uncertainty is multisensory integration (MSI), which is defined as the process of combining information coming from multiple sensory streams to form a new percept with reduced ambiguity (Stein and Stanford, 2008). MSI has been extensively documented in animals from nematodes to humans and in a broad range of behavioral contexts (Wallace et al., 1998; Metaxakis et al., 2018; Zhou et al., 2019; Gil-Guevara et al., 2022). In the context of escape behaviors, MSI of threat-like stimuli increases the escape probability and reduces the latency of the evoked response (Rowland et al., 2007; Martorell and Medan, 2022). In mammals, activation of different parts of the superior colliculus determines whether animals engage in exploratory or defensive behaviors (Dean et al., 1989; Wei et al., 2015). Importantly, the superior colliculus contains neurons that integrate multisensory stimuli due to synaptic convergence of afferents conveying information from different sensory modalities (Kadunce et al., 2001). These studies established that the effects of MSI are larger when weak or ambiguous stimuli are combined, thus showing an inverse effectiveness relationship with stimulus strength. The underlying hypothesis is that integration of sensory signals from different modalities form a more accurate world percept only if each unisensory signal carries some uncertainty or ambiguity.

In goldfish, audiovisual MSI increases the probability and reduces the latency of startle escape behaviors, with an inverse relationship between the MSI effectiveness and the stimulus salience (McIntyre and Preuss, 2019; Martorell and Medan, 2022). These startle escapes (C-starts) are triggered by a pair of reticulospinal neurons (Mauthner cells) that receive visual and auditory inputs through anatomically segregated pathways. Auditory inputs reach the M-cell lateral dendrite through a disynaptic (2 ms) pathway, while the visual inputs relay information in the optic tectum before reaching the M-cell ventral dendrite through a polysynaptic (20 ms) pathway (Zottoli et al., 1987; Pereda et al., 2004; Korn and Faber, 2005; Szabo et al., 2007). Interestingly, the auditory and visual M-cell dendrites show differences in their cable properties, which appear to be well suited to process inputs from abrupt (i.e. fast raise time) auditory pips and more gradually raising visual looms (Medan et al., 2017). However, it is unclear how auditory and visual signals are integrated at the level of the M-cell to generate a multisensory response.

The accessibility of M-cells for *in vivo* intracellular recordings provides an excellent opportunity to investigate the cellular mechanisms of multisensory integration. Moreover, the one-to-one relationship between a single M-cell action potential and the initiation of a C-start (Zottoli, 1977; Weiss et al., 2006; Zwaka et al., 2022) provides a clear link between behavior and the observed integration in the M-cell. As such, the goal of this study was to reveal the cellular mechanism that underlie the multimodal integration of M-cell initiated startle escapes we observed in the behavioral experiments (McIntyre and Preuss, 2019; Martorell and Medan, 2022). Specifically, we studied how visual and auditory presynaptic pathways and intrinsic membrane properties of the M-cell interact to produce MSI to ultimately enhance threat detection. To this end, we performed intracellular *in vivo* recordings from the M-cell soma using auditory and tectal stimuli with naturalistic dynamics (Preuss et al., 2006; Szabo et al., 2006; Medan et al., 2017). Our results show that the temporal dynamics and strength of stimuli, as well as sensory evoked feed-forward inhibition affect the magnitude of MSI. The results represent a rare characterization of MSI at a single-cell level in a neuron that is sufficient and necessary to trigger a distinct behavior.

## METHODS

### Animals

We used adult goldfish (*Carassius auratus*) of both sexes and 7–10 cm of standard body length. Fish were purchased from Billy Bland Fishery (Taylor, AR, USA), Hunting Creek Fisheries (Thurmont, MD, USA) or Daniel Corriarello Aquarium (Buenos Aires, Argentina) and allowed to acclimate for at least a week after transport. Fish were kept in rectangular Plexiglas holding tanks (30 x 60 x 30 $cm^3$; 54 l) in groups of up to 10 individuals. Tanks were supplied with filtered and dechlorinated water and maintained at 18 °C. Ambient light was set to a 12-h light/dark photoperiod. Animals were fed floating pellets (Sera, Germany) five times a week. All procedures and protocols were performed in accordance with the guidelines and regulations of the Institutional Animal Care and Use Committee of Hunter College, City University of New York and Facultad de Ciencias Exactas y Naturales, Universidad de Buenos Aires.

### Auditory stimuli

Sound stimuli consisted in single-cycle sound pips (5-ms duration at 200 Hz) produced by a function generator (33210A Agilent Technologies Inc., Santa Clara, CA, USA) connected to a shielded subwoofer (SA-WN250 Sony Corp., Tokyo, Japan) located 30 cm to the right from the recording chamber. Sound stimuli were recorded with a microphone (XM8500, Behringer) positioned 10 cm over the head of the fish. Calibration recordings were performed with a hydrophone (SQ01, Sensor Technology, Ontario, Canada) positioned where the submerged fish was placed during experiments. Since we were interested in studying integration of subthreshold stimuli, we used sound intensities known to be subthreshold for evoking behavioral startle responses (Neumeister et al., 2008; Weiss et al., 2009; Martorell and Medan, 2022). For all experiments we used a sound intensity of 118 dB SPL (relative to 1 $\mu$Pa in water), except for the experiments in Figure 4 where we used a sound intensity of 147 dB SPL (relative to 1 $\mu$Pa in water). Post-hoc analysis of the M-cell responses in this study revealed that only 3 out of 60 M-cells (5%) fired at least once to an auditory stimulus.

### Optic tectum stimulation

Tectal stimuli were administered to the mid-anterior rim of the left tectum using a bipolar electrode (#30202 FHC, Bowdoin, ME, USA) connected to an isolated stimulator (DS2A; Digitimer Ltd, Welwyn Garden City, UK). In most cases, stimulation [100 µs, 0.1-1mA] in this area was effective in driving subthreshold responses (< 4 mV) in the M-cell. To change the strength and dynamics of the tectal stimulation we either used a 60-Hz stimulation train of variable duration (1, 33, 66, 100, 200 ms) or a 100-ms train of variable frequency (1, 33, 100, 200 Hz). We deliberately used tectal stimuli that evoked

M-cell firing with a very low probability (6.7%, 4 out of 60 M-cells tested fired at least once to any of the tectal stimuli used).

**Electrophysiology**

M-cell intracellular responses to tectal and acoustic stimuli were studied *in vivo* using standard surgical and electrophysiological recording techniques (Preuss and Faber, 2003; Preuss et al., 2006; Medan et al., 2017). To initiate anesthesia, fish were immersed in 1 liter of ice water with 40 mg/l of the general anesthetic tricaine methanesulfonate (MS-222, Western Chemical, Ferndale, WA, USA), until the fish ceased to swim, lost equilibrium and were unresponsive to a pinch on the tail (typically 10–15 min). They were next treated with 20% benzocaine gel (Ultradent, South Jordan, UT, USA) at incision sites and pin-holding points 5 min prior to surgical procedures. Fish were stabilized in the recording chamber by two pins, one on each side of the head, and ventilated through the mouth with recirculating, aerated saline at 18°C (saline [g/l]: sodium chloride 7.25, potassium chloride 0.38, monosodium phosphate monobasic 0.39, magnesium sulfate 0.11, Hepes 4.77; calcium chloride 0.24; dextrose 1.01, pH 7.2). The recording chamber was mounted inside an opaque, thin-walled tank filled with saline that covered the fish up to eye level. The recirculating saline also included a maintenance concentration of the anesthetic MS-222 (20 g/l) that does not interfere with auditory processing (Palmer and Mensinger, 2004; Cordova and Braun, 2007). Next, the spinal cord was exposed with a small lateral incision at the caudal midbody. Bipolar stimulation electrodes were placed on the unopened spinal cord to transmit low-intensity (5–8 V) electrical pulses generated by an isolated stimulator (A 360, WPI, Sarasota, FL, USA). This allowed antidromic activation of the M-cell axons, as confirmed by a visible muscular contraction (twitch). Surgical procedures were performed before a muscle paralysis agent was injected, which allows monitoring the effectiveness of the anesthetic by watching for an increase of opercula movement frequency (largely reduced in deep anesthesia) and movements/twitches in response to the surgical procedures. Shortly before the recordings started, animals were injected I.M. with D-tubocurarine (1 $\mu$g g−1 b.w.; Abbott Laboratories, Abbott Park, IL, USA) and a small craniotomy exposed the medulla for electrophysiological recordings. Antidromic stimulation produces a negative potential in the M-cell axon cap (typically 15–20 mV), which unambiguously identifies the axon hillock and allows intracellular recordings from defined locations along the M-cell soma-dendritic membrane (Furshpan and Furukawa, 1962; Furukawa, 1966; Faber and Korn, 1989). Intracellular recordings were acquired using borosilicate glass electrodes (7–10 M$\Omega$) filled with 5 M potassium acetate and an Axoclamp-2B amplifier (Axon Instruments, Foster City, CA, USA) in current-clamp setting. M-cell responses were acquired with a Digidata 1440A (Axon Instruments) at 25 kHz. Electrodes were advanced using motorized micromanipulators (MP-285;

149 Sutter Instruments, Novato, CA, USA) until reaching the axon cap (defined as a site with an
150 extracellular M-cell AP field >10 mV). Next, the electrode was moved 50 $\mu$m lateral and 50 $\mu$m
151 posterior to penetrate the somatic region. Only trials in which the resting membrane potential was
152 between -90 and -70 mV were included in the analysis.

153 **Statistical Analyses and Experimental Design**

154 To perform statistical analysis, we used R (version 4.0.2, www.r-project.org) and RStudio (version
155 1.1.456, www. rstudio. com). A significance level of $\alpha$ = 0.05 was used throughout the study. Effects
156 of explanatory variables over response variables were assessed using Linear Models followed by
157 ANOVA or binomial GLMs in the case of binary variables. Paired T-tests were used to compare tectal
158 or auditory responses recorded in left or right M-cells (see Fig. 1). Two tailed Wilcoxon Ranked Sum
159 tests were used for single sample comparisons. Sample size is denoted by N when it refers to the
160 number of goldfish, *n* when it refers to the number of trials (average of 5-10 presentations). In
161 experiments where we recorded from both M-cells of the same animals, results were pooled. Boxplots
162 show the median, 25 and 75$^{th}$ percentile, and lines indicate minimum and maximum values.

163 Postsynaptic responses to acoustic and tectal stimuli were recorded at the M-cell soma and averages
164 of 5-10 responses were used in the statistical analysis. M-cell responses to trains of tectal stimulation
165 consist of phasic postsynaptic potentials riding on top of a tonic depolarizing response (Figure 1A-C).
166 We analyzed the contribution of the phasic and tonic components separately (Figure 1A´). To do this
167 we considered a 12 ms window following the last tectal pulse (color-shaded areas in Figure 1A-C) and
168 defined the tonic response amplitude as the difference between the membrane potential immediately
169 before the arrival of the last pulse (blue bar on Figure 1A´) and resting membrane potential. The phasic
170 response was defined as the difference between the peak voltage in response to the last train pulse
171 and the depolarization reached immediately before the last tectal pulse (orange bar on Figure 1A´).

172 To characterize multisensory integration, we quantified responses calculating the mean evoked
173 depolarization in a 12 ms window after sound onset (auditory only trials, A) or after the last tectal
174 stimulus in tectal-only (tectal only trials, T) and multisensory (tectal + auditory trials, M) trials (Fig. 2),
175 considering both phasic and tonic components. We also measured the peak amplitude of the
176 response, which in all cases occurred in the same time window. As peak amplitude analysis resulted
177 in the same qualitative results, only the mean area analysis is shown.

178 For quantification, the responses to M stimuli were normalized to the T and A components. In the field
179 of multisensory integration, multisensory responses are typically normalized to the maximum

response of the unisensory stimulus (Meredith and Stein, 1983; Stanford and Stein, 2007; Stein and Stanford, 2008), which we call Multisensory-Maximum Unimodal index (MSI/Max):

$$MSI/Max = M \div max(T, A)$$

The value of this index determines the net effect of the integration, where M is the multisensory response and max(T, A) is the largest of the two unisensory components (all evaluated as the area in a 12-ms window as defined above). Therefore, a *MSI/Max* greater than 1 represents multisensory enhancement, *MSI/Max* lower than 1 represents multisensory inhibition, and *MSI/Max* not significantly different than 1 suggests absence of multisensory integration (Stein and Stanford, 2008). Additionally, to calculate the linearity of the multisensory integration performed by the M-cell, we calculated the ratio between the multisensory response and the sum of the unisensory responses, which we call Multisensory-Sum Unimodals index (MSI/Sum):

$$MSI/Sum = M \div (T + A)$$

The value of this index indicates the linearity of the integration, determined by the ratio of the multisensory response M and the sum of the unisensory components, T and A. $MSI/Sum$ greater than 1 representing supralinear integration, $MSI/Sum$ of 1 representing linear integration, and $MSI/Sum$ lower than 1 representing sublinear integration (Stanford et al., 2005).

The M-cell is subject to feedforward inhibition which can be triggered by either auditory or tectal stimuli (Faber and Korn, 1982; Medan et al., 2017). Evoked FFI can be quantified as the amplitude reduction of an antidromically evoked “test” action potential (APtest) after presenting a single auditory pip or a brief tectal train as “conditioning” stimuli of similar strength. Both stimuli evoked comparable peak depolarizations in the M-cell (~5 mV). To test if FFI evoked by auditory or tectal stimuli differed, we evoked the APtest at specific times (2–80 ms) following a sensory stimulus and calculated shunting inhibition as %SI= 100 - APtest/APcontrol ×100, where AP control is the amplitude of the AP without a conditioning stimulus (Figure 3A).

One of the principles that guide multisensory integration is the spatial coherence of the different cues being integrated. If the perceived source localizations of two stimuli overlap, these stimuli are more

likely to be integrated. Conversely, if the two stimuli arrive from spatially disparate sources the chances of observing a multisensory integration will decrease (Meredith and Stein, 1996; Stein and Stanford, 2008). The geometrical configuration of the setup in our experiments determined that the loudspeaker used to produce acoustic stimuli was mounted to the right of the fish and electrical stimulation was applied to the left tectum (which normally receives visual signals from the right retina). Whenever possible, we performed recordings from both Mauthner cells. To rule out the possibility of a systematic difference on the responses of either M-cell due to the spatial source of the stimuli, we compared the responses to tectal or auditory stimuli in sequential recordings of the right and left M-cells of the same fish. Supplementary Figure 1 shows representative trace examples for tectal (100 ms 60 Hz tectal train, Fig. Supp. 1A) and auditory (5 ms 200 Hz auditory pip, Fig. Supp. 1B) stimulation from the left (upper traces) or right (lower traces) M-cell of the same fish. The complex post-synaptic potentials were highly stereotypical in successive presentations of a T or A stimuli within and across cells. Analysis from pairs of tectal (Fig. Supp. 1C, N=9) and auditory (Fig. Supp. 1D, N=11) M-cell responses showed no statistical differences between ipsi- and contralateral stimulation (paired T-test, T: $t(8)= 0.18$, $p=0.8573$, A: $t(10)= -0.76$, $p=0.4672$). This confirms previous results indicating that in goldfish, tectal stimulation produces responses with similar latency and amplitude in both M-cells (Zottoli et al., 1987; Canfield, 2006). We therefore pooled data acquired from left or right M-cells for all following analysis.

229 RESULTS

230

231 **MAUTHNER CELL RESPONSES ARE SENSITIVE TO THE DYNAMICS OF TECTAL STIMULI**

232 Multisensory integration is known to be dependent on the saliency of the unimodal components
233 (Stanford et al., 2005; Martorell and Medan, 2022). To create a stimulus set of variable strength and
234 temporal dynamics, we recorded M-cell responses to different electrical trains delivered in the
235 posterior rim of the tectum. As shown in other species, goldfish adapt rapidly to repeated natural-
236 looming stimulation (Marquez-Legorreta et al., 2022; Fotowat and Engert, 2023). Indeed, in previous
237 behavioral experiments we presented looming stimuli with intertrial intervals (ITI) of about 4-5
238 minutes to reduce such adaptation (Preuss et al., 2006; Otero Coronel et al., 2020; Martorell and
239 Medan, 2022). However, ITI of 4-5 min are prohibitively long for steady intracellular recordings.
240 Considering these restrictions, we used tectal stimuli (that bypass the retina) at an ITI of 30 s which
241 does not produce adaptation. This tectal stimulation results in depolarization responses in the ventral
242 ('visual') dendrite of the M-cell that are qualitatively and quantitatively similar to those elicited by
243 visual looming stimuli. While this approach bypasses retinal and tectal processing of visual inputs, it is
244 important to note that the tectum also integrates multisensory inputs, including from the thalamus
245 and other sensory pathways such as the auditory and vestibular systems. As a result, tectal stimulation
246 is likely to recruit projections that are predominantly, but not exclusively, visual. Nonetheless, tectal
247 afferents reach the distal ventral dendrite of the M-cell and produce non-adapting synaptic responses
248 that retain key characteristics of looming responses such as fast PSPs riding on top of a ramped
249 depolarization (Preuss et al., 2006; Szabo et al., 2006; Medan and Preuss, 2014; Medan et al., 2017,
250 Zottoli et al.,1987) (Figure 1A). M-cell somatic responses reach a plateau after 30-100 ms and decay
251 to resting values 200-300 ms after the end of the tectal train. To characterize how the M-cell responses
252 depend on the frequency and duration of the stimulation trains in the tectum, we recorded responses
253 to 60-Hz trains that varied in duration (Figure 1A-B, N=18), and 100-ms tectal trains that varied in pulse
254 frequency (Figure 1C-D, N=11). The responses to both sets of trains exhibited complex temporal
255 dynamics with a tonic component that progressively builds during the train and a fast phasic
256 component after each pulse (Figure 1A').

257 Increasing the duration of the 60-Hz trains drove stronger tectal responses due to the increase of the
258 tonic component of the response while the phasic response remained unchanged (ANOVA, tonic: $F(3, 40)=37.29$, $p<0.0001$, phasic: $F(3,40)=0.58$, $p= 0.6311$, Figure 1B). Increasing the frequency of the 100-
260 ms stimulation trains also drove stronger tectal responses due to a large increase in the tonic

261 component (ANOVA, tonic: $F(3, 30)=12.29$, $p<0.0001$). However, increasing the tectal stimulus
262 frequency produced a significant reduction in the amplitude of the phasic component (ANOVA, phasic:
263 $F(3, 30)=11.29$, $p<0.0001$, Figure 1D). Comparing the stimulus trains of variable duration and
264 frequency reveals that modifying the duration of the 60-Hz trains or the frequency of 100-ms trains is
265 similarly effective in tuning the magnitude of the responses. Increasing the duration of a 60 Hz from
266 33 to 200 ms produced a 45% increase in the total response amplitude (phasic + tonic) while increasing
267 the frequency from 30 to 200 Hz produced a 50% increase in the response amplitude (Figures 1 B, D).
268 Since multimodal integration is known to depend on the strength of the unimodal components
269 (Stanford et al., 2005; Martorell and Medan, 2022), in the following multimodal experiments we
270 leveraged this characterization to generate tectal stimuli of variable strength and dynamics. Although
271 both the 60-Hz trains of variable duration and the 100-ms trains of variable frequency evoked
272 responses of similar total amplitude, we decided to include both sets of trains in our multisensory
273 stimuli to determine whether any detected effect depended on the temporal structure of the stimulus
274 or the ratio of phasic-to-tonic responses.

275 **MULTISENSORY ENHANCEMENT IN THE MAUTHNER CELL**

276 Abrupt sound stimuli have been extensively used to trigger the short latency escape responses
277 initiated by firing of the M-cell (Eaton et al., 1977; Burgess and Granato, 2007; Neumeister et al., 2008;
278 Weiss et al., 2009; Zheng and Schmid, 2023). Acoustic stimulation produces a complex response in the
279 M-cell which is composed of a fast EPSP superimposed on a depolarizing envelope termed slow EPSP
280 (Szabo et al., 2006). The fast EPSP is composed of fast electrical coupling potentials resulting from
281 firing of the 8th nerve auditory afferences that synapse the distal end of the lateral dendrite of the M-
282 cell (club endings) (Pereda et al., 2004; Szabo et al., 2007). In contrast, the slow EPSP is originated by
283 chemical (glutamatergic) synaptic contacts on the soma and proximal dendrite conveying information
284 from inner hear endorgans and it has been shown that it mostly carries information on stimulus
285 intensity (Szabo et al., 2006). Although the M-cell is known to respond to stimuli of different
286 modalities, there are no reports on how it combines and integrates information when auditory and
287 tectal sources are co-presented. To determine whether multisensory enhancement occurs in the M-
288 cell, we recorded somatic responses to an auditory pip (unisensory auditory, A), a tectal stimulation
289 train (unisensory tectal, T), and their combination (multisensory audiotectal, M) (Figure 2A, E).

290 Increasing the duration of the 60-Hz tectal train positively modulated the multisensory responses
291 (amplitudes ranging from 3.08 ± 0.84 mV to 5.29 ± 1.64 mV, N=17, n=47; LM: evoked depolarization
292 ~ tectal duration, $F(1,45)=17,39$, $p=0.0001$, Figure 2B). We then compared the multisensory responses
293 to their unisensory counterparts. When M responses were normalized to the most effective

294 unisensory response, multisensory stimuli yielded MSI/Max indices that ranged from 1.48 to 1.53 for
295 all stimulus durations (Wilcoxon single sample test mu=1, alternative mu≠1, p<0.001 for all stimulus
296 durations, Figure 2C), indicating a significant multisensory enhancement of the response. When the
297 M response was normalized to the sum of both unisensory responses, the MSI/Sum indices were lower
298 than 1 (i.e. sublinear integration, Wilcoxon single sample test mu=1, alternative mu≠1, p<0.01) for all
299 cases except for the briefest tectal stimulus, for which the MSI/Sum index was 1.06 (i.e. linear
300 integration, Wilcoxon single sample test mu=1, alternative mu≠1, p<0.0676, Figure 2D).

301 Increasing the frequency of a 100-ms tectal train (Figure 2E) was not as effective in modulating the
302 multisensory responses (LM: evoked depolarization ~ tectal frequency, F(1,39)=3.96, p=0.0535, Figure
303 2F). However, the M responses still exhibited MSI/Max indices that ranged 1.43-1.53 when compared
304 to the largest unimodal stimulus (Figure 2G) indicating that a 100 ms tectal train (irrespective of its
305 frequency) significantly enhances the M-cell response. The MSI/Sum of these M responses ranged
306 0.82 to 0.86 showing a similar sublinear integration to that of the multisensory stimuli with the longer
307 60-Hz trains (Wilcoxon single sample test mu=1, alternative mu≠1, all p≤0.01, Figure 2H). Neither
308 MSI/Max or MSI/Sum showed a significant dependency with tectal frequency (LM: MSI/Max ~ tectal
309 frequency, F(1,39)=0.02, p=0.882, MSI/Sum ~ tectal frequency, F(1,39)=0.49, p=0.487).

310 Overall, these results show that, in all cases, combining an auditory pip with a preceding tectal pulse
311 enhances the M-cell response by about 50%. This multisensory enhancement does not show a strong
312 modulation by the duration or frequency of the tectal stimulus (Figure 2C, G). However, while most
313 multisensory stimuli exhibited a sublinear integration, the multisensory stimulus with the shortest
314 (and weakest) tectal component produced a linear response (Figure 2B, D).

315 **TECTAL- AND AUDITORY-EVOKED FEEDFORWARD INHIBITIONS EXHIBIT DISTINCT TEMPORAL**
316 **DYNAMICS**

317 Both visual and auditory stimuli evoke feedforward inhibition (FFI) at the perisomatic region of the M-
318 cell through a population of inhibitory interneurons which open chloride channels that produce
319 shunting of the postsynaptic currents (Diamond et al., 1973; Zottoli et al., 1987; Koyama et al., 2011;
320 Tabor et al., 2018). This FFI restricts the temporal window of sensory excitation to terminate the
321 excitatory signal. In combination with passive membrane decay, an increase in FFI will further narrow
322 the window for temporal integration. Conversely, a decrease in FFI would increase the lingering
323 depolarization of a response produced by a previous stimulus, and thus extend the temporal
324 integration window. These differences in the strength or temporal dynamics between visual and
325 auditory evoked FFI may affect multisensory integration (Felch et al., 2016).We used a single auditory

326 pip and a brief tectal train as “conditioning” stimuli of similar strength, which evoked comparable peak
327 depolarizations in the M-cell (~5 mV) (Figure 3A). Peak FFI inhibition induced by auditory and tectal
328 stimulation showed similar amplitude (Figure 3B, auditory vs. tectal %SI: 13.65 ± 4.74 vs. 14.55 ± 7.50;
329 Kruskal-Wallis chi-squared (1)= 0.01, p = 0.9066, N=19) with peak inhibition at the same time (auditory
330 vs. tectal time (ms) of maximum %SI: 9.04 ± 3.93 vs. 8.85 ± 6.54; Kruskal-Wallis chi-squared(1)= 0.30,
331 p = 0.5838, Figure 3C, N=19). In a subset of experiments (N = 7), both auditory and tectal FFI were
332 evaluated sequentially in the same cell and same recording site which allowed us to have an accurate
333 estimate of the inhibition triggered by each sensory modality (Figure 3D). Although the maximum level
334 of inhibition was comparable and was reached in a similar time, recovery from inhibition was much
335 faster for tectal than for auditory FFI. Tectal FFI decayed to 50% of its peak in 8 ms, compared to 30
336 ms for the auditory FFI (Kruskal-Wallis chi-squared (1)= 5.97, p =0.0145, Figure 3E). In addition, the
337 area under the curve for auditory FFI was almost 3 times greater than for tectal FFI (502 vs. 176 %*ms,
338 respectively, Kruskal-Wallis chi-squared (1)= 5.58, p = 0.0181, Figure 3F).

339 These results highlight the key role of the temporal dynamics of the inhibition that reaches the M-cell
340 and which in turn will affect integration in the M-cell. Moreover, these results show that auditory
341 stimuli trigger more prolonged inhibition than tectal stimuli of similar amplitude and decay time. The
342 short-lived FFI that follows tectal stimulation suggests that multiple trains or waves of tectal inputs
343 are more likely to be integrated and summed than multiple sounds. This goes in line with the duration
344 of visual looms that are most effective in triggering the M-cell and eliciting visual C-start escapes
345 (Preuss et al., 2006; Temizer et al., 2015). Differences on the decay rate of inhibition produced by brief
346 tectal or auditory stimuli could affect integration of pairs of brief sensory stimuli depending on their
347 sequence and their timing, which is explored in the next section.

348 **STIMULUS TEMPORAL ORDER AND MODALITY AFFECT STIMULI INTEGRATION**

349 There are several anatomical and functional differences in the pathways followed by auditory and
350 visual inputs that eventually reach the M-cell soma. First, auditory inputs from the 8$^{th}$ nerve reach the
351 distal lateral dendrite of the M-cell through a disynaptic (≈2 ms) pathway followed by slower inputs
352 from glutamatergic synaptic contacts on the soma and proximal dendrite**.** Visual inputs reach the
353 ventral dendrite after a polysynaptic (≈20 ms) pathway that includes the optic tectum (Zottoli et al.,
354 1987; Szabo et al., 2006). Second, M-cell dendritic characteristics determine modality specific filtering
355 differences resulting in stronger attenuation of visual than auditory signals (Medan et al., 2017). For
356 auditory stimuli, it has been reported that a sound pip that precedes by 20-150 ms a second sound
357 reduces the M-cell response to the second sound, a phenomenon known as auditory prepulse
358 inhibition (Neumeister et al., 2008; Curtin and Preuss, 2015; Tabor et al., 2018). However, it is unclear

359 whether a similar inhibitory integration would hold true for cross-modal and tectal-tectal interactions,
360 since auditory and visual inputs travel through distinct and separated pathways and undergo different
361 filtering.

362 To investigate the role of input modality on M-cell integration we used pairs of similarly brief (~10 ms)
363 auditory pips and tectal pulses 50 ms apart with in all possible sequences, including unisensory
364 combinations (AA, TT) and multisensory combinations (AT, TA, Figure 4, N= 29, n= 50). We decided to
365 use a 50 ms interval because it was observed to be a period after which the tectal FFI had returned to
366 baseline values, while the auditory FFI remained at about 4%. The amplitude of the tectal stimulation
367 pulse was chosen so that the M-cell responses to the tectal and auditory stimuli were of similar
368 magnitude (4-8 mV). The initial response to the first stimulus (S1, auditory in the example shown in
369 Figure 4A, top trace) decayed passively over the course of 50 ms, and at that point the second stimulus
370 was presented (S2, tectal in the example shown if Figure 4A, bottom trace). The mean lingering
371 depolarization remaining immediately before the second stimulus was delivered (Figure 4A, top trace,
372 pink bar) was slightly larger for the evoked auditory pip than for the tectal stimulus (Figure 4B, A: 1.48
373 ± 0.79mV vs. T: 0.95 ± 0.50mV, Kruskal-Wallis rank sum test (1) = 5.5173, p = 0.0188).

374 We next calculated the integration indices of the four possible combinations of uni and multisensory
375 pairs (AA, AT, TA, TT). For that, we measured the depolarization in A-only or T-only trials in 12-ms
376 windows. These windows started either 50 ms after stimulus onset to account for the contribution of
377 the first stimulus, S1 (Figure 4A, Resp1, orange area of top trace), or immediately after stimulus
378 presentation to account for the contribution of the second stimulus, S2 (Figure 4A, Resp2, green area
379 of middle trace). Then, we measured the response for pairs of stimuli in a 12-ms window after the
380 presentation of S2 (Figure 4A, Resp(1+2), bottom trace). Finally, we calculated the integration for each
381 type of uni (AA and TT) or multisensory stimuli (AT and TA) defining a "S1-S2 Integration Index" as S1-
382 S2 Int./Sum= Resp(1+2)/(Resp1 + Resp2)). Note that for multisensory trials (i.e. AT or TA), this metric
383 is equivalent to the MSI/Sum index, except for a 50-ms temporal offset in the presentation and
384 quantification of the first stimulus.

385 In the AA trials (N=21) we observed an inhibitory integration (S1-S2 Int./Sum < 1, two-sided Wilcoxon
386 rank test, p<0.0001) with the first auditory pip reducing the amplitude expected for the second pip by
387 42%, as others have previously described (Neumeister et al., 2008; Curtin and Preuss, 2015; Tabor et
388 al., 2018). The AT combination also showed sublinear integration (S1-S2 Int./Sum < 1, two-sided
389 Wilcoxon rank test, p = 0.0078) while the TT and TA combinations showed linear integration (S1-S2
390 Int./Sum =1, two-sided Wilcoxon rank test, VA: p = 0.0681, VV: p = 0.9453, Figure 4C). The inhibitory

391 effect in the AA combination was significantly larger than for the AT combination (Figure 4C, 1w-
392 ANOVA, F=38.34, p<0.0001).

393 **MULTISENSORY INTEGRATION IN THE MAUTHNER CELL SHOWS INVERSE EFFECTIVENESS**

394 The principle of inverse effectiveness states that the effects of multisensory integration are typically
395 larger when the components of a multisensory stimulus are weak. Throughout our experiments, we
396 only observed linear integration of multisensory stimuli when presenting single tectal pulses (Figure
397 2C, 1ms tectal), or brief (~10 ms) trains (Figure 4, AT – TA), and observed sublinear integration for
398 multimodal stimuli with longer tectal trains (Figure 2D-H). However, these results represent the
399 average MSI for each group for a specific set of experimental conditions and effectively simplify the
400 diverse range of responses across trials, experimental conditions, and fish. To compare the overall
401 dependence of the multisensory enhancement on the strength of sensory inputs, we pooled the
402 multisensory integration indexes for experiments irrespective of sequence of stimuli (AT and TA, N=18,
403 n=174), tectal train duration (from a single 1-ms tectal pulse to a 200-ms train) and frequency (from a
404 single pulse to 1000Hz) (Figure 5A, MSI/Max and B, MSI/Sum). We found a significant inverse
405 correlation between the magnitude of the multisensory enhancement and the magnitude of the
406 unisensory components (MSI/Max, LM, F(1,172): 28.17, p<0.0001; MSI/Sum, LM, F(1,172): 67.33,
407 p<0.0001). This result parallels the inverse effectiveness reported at the behavioral level in goldfish
408 (McIntyre and Preuss, 2019; Martorell and Medan, 2022), confirming that the relative multisensory
409 enhancement obtained by combining two inputs is proportionally higher when the stimuli are weak.
410 Combinations of weak stimuli (<2.5mV, Figure 5B) produce supralinear multisensory responses that
411 are between 50-100% stronger than the most effective unisensory stimulus (Figure 5A). Noteworthy,
412 these results provide robust evidence that in the escape network of fish, inverse effectiveness of
413 multisensory integration is implemented, at least, at the single (Mauthner) cell level.

414 Although the previous analysis was based on subthreshold responses, in a low proportion of
415 experiments M-cells fired in response to sensory stimulation. Of 60 M-cells tested, 3 (5%) fired to
416 auditory, 4 (6.7%) to tectal, and 7 (11.7%) to multimodal stimuli. The low firing chance is likely due to
417 the fact that our in vivo recordings were performed in anesthetized and paralyzed animals. Although
418 not statistically significant due to the low number of events (Pearson's chi-squared test X2: 0.40,
419 p=0.5269), these data show a tendency to a higher response probability to multisensory than
420 unisensory stimuli. Figure 5C shows two "proof-of-concept" examples from two different animals in
421 which the M-cells showed subthreshold responses to unisensory stimuli and elicited an action
422 potential when the two stimuli are combined. Since an action potential in the M-cell triggers the
423 initiation of a C-start escape, these are examples of behaviors that only occurred in response to a

multisensory stimulus but not to either of the unisensory components. This highlights how, because of the all-or-nothing nature of action potentials, relatively small increments in the M-cell response due to multisensory enhancement could be sufficient to make the cell trigger and have a profound effect in escape behavior, even if the integration is sublinear.

429 DISCUSSION

430 The Mauthner-cell system triggers a behavior of vital importance: escaping from predators. A
431 combination of fast afferent circuits, synaptic specialization, special intrinsic properties and topology
432 of the M-cell contribute in concert to a fast startle escape response (Eaton et al., 1991; Korn and Faber,
433 2005). Here we show that the M-cell incorporates multisensory information to enhance its responses
434 and characterize how the integration of multiple stimuli is affected by the modality, spatial source,
435 temporal structure, temporal order, and intensity of the stimuli. Although multisensory enhancement
436 has been previously described in different neural populations and across a wide range of species, it
437 was unclear whether the activity of these neurons was necessary, sufficient, or even influenced the
438 execution of behavioral responses to multisensory stimuli. In contrast to other known multisensory
439 structures of vertebrates multisensory integration in the M-cell has an unequivocal function in fish
440 behavior and survival, as it directly determines whether and when a C-start is triggered (McIntyre and
441 Preuss, 2019; Martorell and Medan, 2022) .

442 Different factors differentially affect the summation and integration of auditory and visual inputs to
443 the M-cell. First, sensory inputs are subject to different passive decays depending on the site of the
444 dendritic arbor at which they arrive. Auditory inputs reach the M-cell distal lateral dendrite through
445 dense mixed electrical and chemical synapses driven through the posterior 8th-nerve afferents and
446 the proximal dendrite through indirect glutamatergic inputs conveying information from inner ear
447 endorgans (Szabo et al., 2006, 2007). In contrast, visual inputs arriving to the ventral dendrite establish
448 synapses that do not show additional specializations as the club endings (Zottoli et al., 1987; Cachope
449 et al., 2007; Szabo et al., 2007). Second, the geometrical properties of the M-cell lateral and ventral
450 dendrites (length and tapering) impose different filters on the input signal which determine a stronger
451 spatial decay for visual than for auditory signals (Medan et al., 2017). Third, as excitatory (and
452 inhibitory) signals reach the soma, the active ion conductances decrease the membrane resistance
453 and impact the response to following signals (Hodgkin, 1947). Finally, the magnitude and dynamics of
454 the stimuli will also affect integration. Both abrupt auditory pips and longer lasting auditory looms
455 generate fast EPSPs that depend on the stimulus frequency and a depolarizing envelope proportional
456 to the stimulus amplitude (Szabo et al., 2006) that slowly decays to baseline (Figure 4). Although the
457 pathways for auditory and visual inputs are completely different, tectal responses also consist of fast
458 peaks that track stimulus frequency and a tonic depolarizing envelope proportional both to stimulus
459 duration and frequency (Figure 1) that also decays slowly (Figure 4).

460 These temporal dynamics of the responses modulate the effective multisensory integration in the M-
461 cell soma, which emerges as a complex, nonlinear interaction between “positive” (input strength and

462 summation, voltage dependent depolarizing conductances) and “negative” (temporal and spatial
463 decay, feedforward inhibition, and depolarization-induced decrease in input resistance) contributions.
464 These factors likely influence integration in any multisensory neuron. However, the accumulated
465 knowledge on the presynaptic pathways and the intrinsic mechanisms operating in the M-cell
466 combined with its functional role in commanding the initiation of the C-start response makes this
467 neuron a unique model for analyzing multisensory integration in a single identifiable neuron.

468 We have previously shown that fish exhibit a behavioral multisensory enhancement of the C-start
469 escape response for audiovisual stimuli, and that this effect is reduced when increasing the salience
470 of the unisensory stimuli (Martorell and Medan, 2022). Therefore, one of our goals here was to
471 investigate if the inverse effectiveness principle observed behaviorally had its correlation in
472 integration processes taking place in the M-cell. Paralleling our previous behavioral results, here we
473 show through intracellular recordings that the response evoked by an auditory pip can be increased
474 by about 50% when it is preceded by a tectal stimulus (Figure 2C, G). This enhancement was not
475 affected by relatively large changes in stimulus frequency. The plateau in the tonic depolarization
476 observed 30-50 ms after a sustained stimulus (Figure 1A) combined with the low-pass filtering
477 properties of the membrane could be responsible for the lack of frequency effects. These two
478 mechanisms point to the M-cell role as a “sudden” stimulus detector rather than a precise coder of
479 sensory stimulus properties.

480 When we combined a tectal train with an auditory pip to obtain a multisensory stimulus, the response
481 was smaller than the sum of the evoked depolarization of the two components (Figures 2D, H). This
482 sublinear effect was expected in the case of passive integration, since cellular biophysics predict a
483 sublinear integration of subthreshold inputs due to a reduction in the driving force of sodium and the
484 aperture of ion channels that reduce the membrane resistance. Noteworthy, action potentials are all-
485 or-nothing events, so the effects when the membrane potential is close to the threshold, sublinear
486 summation can determine that an otherwise silent neuron fires an AP (Figure 5C). Therefore, a weak
487 (subthreshold) auditory pip combined by a weak visual stimulus in close temporal association might
488 be sufficient for triggering an escape response. Indeed, analysis of 60 M-cells tested with A, T and M
489 stimuli showed that auditory stimuli evoked firing in 5% of cells, tectal stimuli in 6.7% of cells but
490 almost 12% of M-cells fired in response to multisensory stimuli. Even though these results are
491 probably an underestimation of actual firing probabilities due to anesthesia and paralyzing agents,
492 they provide a mechanistic support to our previous behavioral observations (Martorell and Medan,
493 2022).

494 Importantly, for the weakest multisensory stimuli the M-cell response deviated from this sublinear
495 integration (Figures 2C and 5A). When the sum of unisensory components is less than 2.5 mV
496 (essentially a single tectal stimulus immediately followed by a single auditory pip) summation is linear
497 (Figure 2D and 5A). This suggests the existence of one or more active mechanism/s of multisensory
498 integration upstream of the M-cell soma, potentially through a presynaptic neuron that also receives
499 audiovisual inputs and projects to the M-cell or locally at the level of the dendritic tree of the M-cell.
500 Moreover, previous work has described that the M-cell membrane non-linearities in the lateral and
501 ventral dendrites which progressively increase M-cell excitability for depolarizations above 5 mV
502 (Faber and Korn, 1986; Medan et al., 2017). Such nonlinear properties might enhance multisensory
503 integration of weak stimuli (Martorell and Medan, 2022) providing a cellular mechanism for the
504 principle of inverse effectiveness of multisensory integration.

505 The temporal structure of the multisensory stimuli is crucial to allow the animal to effectively "bind"
506 or associate both signals as coming from a single source (Stein and Stanford, 2008). In the M-cell, this
507 translates into the time window where the effect on the membrane voltage (excitatory or inhibitory)
508 persists. Here, we found that a delay of 50 ms between the components of a low-amplitude
509 multisensory stimuli result in a linear summation of the signals (Figure 4C) and that the temporal order
510 of the components produces a slight effect in the integration (Figure 4C, AT vs. TA) (Felch et al., 2016).
511 As it has been previously suggested, the lengthy decay of the slow EPSP of the auditory pip (or the
512 tonic component of the tectal train) probably contributed to relax the requirement for coincident
513 inputs, effectively broadening the temporal window of integration (Szabo et al., 2006). On the other
514 hand, the integration of unisensory stimuli was dependent on the modality of the stimuli: two tectal
515 (TT) stimuli summed linearly while two auditory (AA) stimuli summed sublinearly (Figure 4C). This
516 difference might be due to differences in both the presynaptic networks that mediate PPI (Tabor et
517 al., 2018) and in the temporal decay of auditory and tectally evoked FFI (Figure 3D). Auditory stimuli
518 produce a longer-lasting inhibition than tectal stimuli of similar strength (Figure 3F) and while tectal
519 inhibition is almost extinct 50 ms after a tectal stimulus, auditory inhibition stabilizes at around 50%
520 of the maximum inhibitory effect in a time window of 30 to 70 ms after an auditory stimulus (Figure
521 3E). Interestingly, the integration of AT stimuli was smaller than that of TA, supporting a differential
522 cross-modal and intra-modal integration of the excitatory or inhibitory components (Figure 4C).
523 Another factor that could be contributing to the differential integration between AA and AT stimuli is
524 that FFI inhibition is likely to be heterogeneously spread in the perisomatic area around the M-cell. If
525 auditory stimulation recruits inhibitory PHP neurons that target the proximal lateral dendrite of the
526 M-cell, a subsequent sensory input propagating along the lateral dendrite (i.e, auditory input) would
527 suffer stronger attenuation than one reaching the soma through the ventral dendrite (i.e., tectal

input). However, specific studies are required to test this hypothesis as it is still unclear if auditory and tectal afferent fibers synapse the same or different sets of inhibitory neurons and which is the spatial distribution of those inhibitory contacts. Additionally, presynaptic elements could also contribute to the asymmetry in unimodal auditory (AA) vs. unimodal tectal (TT) or multisensory processing. A subset of glutamatergic Gsx1 neurons located in rhombomere 4 have been shown to mediate M-cell auditory presynaptic inhibition (Tabor et al., 2018). These neurons produce presynaptic inhibition of 8$^{th}$ nerve auditory fibers adjacent to the distal portion of the M-cell lateral dendrite but leave unaffected the ventral dendrite. This mechanism could therefore affect the processing of pairs of sensory signals that initiate with an auditory component (AA, AT) and leave the integration of tectal or multisensory stimuli unaffected.

ACKNOWLEDGEMENTS

This work was supported by PICT 2012-1578 and PICT 2017-0007, FONCYT-ANPCYT (VM), PIP 11220130100729CO (VM), UBACyT 20020130300008BA (VM), Thalmann Program, University of Buenos Aires (VM) SOC was supported by undergraduate fellowships from the National Interuniversity Council and University of Buenos Aires. The authors thank Dr. Lidia Szczupak and members of the Medan lab for discussion and for reading previous versions of this manuscript. The current address of SOC is at The Rockefeller University, New York, NY, USA (10065).

AUTHOR CONTRIBUTIONS

SOC, TP and VM conceived the research. SOC and VM performed experiments and analyzed the data. SOC and VM wrote the manuscript.

549 REFERENCES


550 Burgess HA, Granato M (2007) Sensorimotor gating in larval zebrafish. J Neurosci 27:4984–4994.

551 Cachope R, Mackie K, Triller A, O'Brien J, Pereda AE (2007) Potentiation of electrical and chemical
552 synaptic transmission mediated by endocannabinoids. Neuron 56:1034–1047.

553 Canfield JG (2006) Functional evidence for visuospatial coding in the Mauthner neuron. Brain Behav
554 Evol 67:188–202.

555 Cordova MS, Braun CB (2007) The use of anesthesia during evoked potential audiometry in goldfish
556 (Carassius auratus). Brain Res 1153:78–83.

557 Curtin PCP, Preuss T (2015) Glycine and GABAA receptors mediate tonic and phasic inhibitory
558 processes that contribute to prepulse inhibition in the goldfish startle network. Front Neural Circuits
559 9:12.

560 Dean P, Redgrave P, Westby GWM (1989) Event or emergency? Two response systems in the
561 mammalian superior colliculus. Trends Neurosci 12:137–147.

562 Diamond J, Roper S, Yasargil GM (1973) The membrane effects, and sensitivity to strychnine, of
563 neural inhibition of the Mauthner cell, and its inhibition by glycine and GABA. J Physiol 232:87–111.

564 Eaton RC, Bombardieri RA, Meyer DL (1977) The Mauthner-initiated startle response in teleost fish. J
565 Exp Biol 66:65–81.

566 Eaton RC, DiDomenico R, Nissanov J (1991) Role of the Mauthner cell in sensorimotor integration by
567 the brain stem escape network. Brain Behav Evol 37:272–285.

568 Faber DS, Korn H (1982) Transmission at a central inhibitory synapse. I. Magnitude of unitary
569 postsynaptic conductance change and kinetics of channel activation. J Neurophysiol 48:654–678.

570 Faber DS, Korn H (1986) Instantaneous inward rectification in the Mauthner cell: a postsynaptic
571 booster for excitatory inputs. Neuroscience 19:1037–1043.

572 Faber DS, Korn H (1989) Electrical field effects: their relevance in central neural networks. Physiol
573 Rev 69:821–863.

574 Felch DL, Khakhalin AS, Aizenman CD (2016) Multisensory integration in the developing tectum is
575 constrained by the balance of excitation and inhibition. eLife 5:e15600.

576 Fotowat H, Engert F (2023) Neural circuits underlying habituation of visually evoked escape
577 behaviors in larval zebrafish Kawakami K, Moore T, eds. eLife 12:e82916.

578 Furshpan EJ, Furukawa T (1962) Intracellular and extracellular responses of the several regions of the
579 Mauthner cell of the goldfish. J Neurophysiol 25:732–771.

580 Furukawa T (1966) Synaptic interaction at the mauthner cell of goldfish. Prog Brain Res 21:44–70.

581 Gil-Guevara O, Bernal HA, Riveros AJ (2022) Honey bees respond to multimodal stimuli following the
582 principle of inverse effectiveness. J Exp Biol 225:jeb243832.

583 Hodgkin AL (1947) The membrane resistance of a non-medullated nerve fibre. J Physiol 106:305–
584 318.

585 Kadunce DC, Vaughan JW, Wallace MT, Stein BE (2001) The influence of visual and auditory receptive
586 field organization on multisensory integration in the superior colliculus. Exp Brain Res 139:303–310.

587 Korn H, Faber DS (2005) The Mauthner cell half a century later: a neurobiological model for decision-
588 making? Neuron 47:13–28.

589 Koyama M, Kinkhabwala A, Satou C, Higashijima S, Fetcho J (2011) Mapping a sensory-motor
590 network onto a structural and functional ground plan in the hindbrain. Proc Natl Acad Sci U S A
591 108:1170–1175.

592 Marquez-Legorreta E, Constantin L, Piber M, Favre-Bulle IA, Taylor MA, Blevins AS, Giacomotto J,
593 Bassett DS, Vanwalleghem GC, Scott EK (2022) Brain-wide visual habituation networks in wild type
594 and fmr1 zebrafish. Nat Commun 13:895.

595 Martorell N, Medan V (2022) Audiovisual integration in the Mauthner cell enhances escape
596 probability and reduces response latency. Sci Rep 12:1097.

597 McIntyre C, Preuss T (2019) Influence of Stimulus Intensity on Multimodal Integration in the Startle
598 Escape System of Goldfish. Front Neural Circuits 13:7.

599 Medan V, Mäki-Marttunen T, Sztarker J, Preuss T (2017) Differential processing in modality-specific
600 Mauthner cell dendrites. J Physiol. 596(4):667-689.

601 Medan V, Preuss T (2014) The Mauthner-cell circuit of fish as a model system for startle plasticity. J
602 Physiol-Paris 108:129–140.

603 Meredith MA, Stein BE (1983) Interactions among converging sensory inputs in the superior
604 colliculus. Science 221:389–391.

605 Meredith MA, Stein BE (1996) Spatial determinants of multisensory integration in cat superior
606 colliculus neurons. J Neurophysiol 75:1843–1857.

607 Metaxakis A, Petratou D, Tavernarakis N (2018) Multimodal sensory processing in Caenorhabditis
608 elegans. Open Biol 8:180049.

609 Neumeister H, Szabo TM, Preuss T (2008) Behavioral and physiological characterization of
610 sensorimotor gating in the goldfish startle response. J Neurophysiol 99:1493–1502.

611 Otero Coronel S, Martorell N, Beron de Astrada M, Medan V (2020) Stimulus Contrast Information
612 Modulates Sensorimotor Decision Making in Goldfish. Front Neural Circuits 14:23.

613 Palmer LM, Mensinger AF (2004) Effect of the anesthetic tricaine (MS-222) on nerve activity in the
614 anterior lateral line of the oyster toadfish, Opsanus tau. J Neurophysiol 92:1034–1041.

615 Pereda AE, Rash JE, Nagy JI, Bennett MVL (2004) Dynamics of electrical transmission at club endings
616 on the Mauthner cells. Brain Res Brain Res Rev 47:227–244.

617 Preuss T, Faber DS (2003) Central cellular mechanisms underlying temperature-dependent changes
618 in the goldfish startle-escape behavior. J Neurosci 23:5617–5626.

619 Preuss T, Osei-Bonsu PE, Weiss SA, Wang C, Faber DS (2006) Neural representation of object
620 approach in a decision-making motor circuit. J Neurosci Off J Soc Neurosci 26:3454–3464.

621 Rowland BA, Quessy S, Stanford TR, Stein BE (2007) Multisensory integration shortens physiological
622 response latencies. J Neurosci Off J Soc Neurosci 27:5879–5884.

623 Stanford TR, Quessy S, Stein BE (2005) Evaluating the Operations Underlying Multisensory
624 Integration in the Cat Superior Colliculus. J Neurosci 25:6499–6508.

625 Stanford TR, Stein BE (2007) Superadditivity in multisensory integration: putting the computation in
626 context. Neuroreport 18:787–792.

627 Stein BE, Stanford TR (2008) Multisensory integration: current issues from the perspective of the
628 single neuron. Nat Rev Neurosci 9:255–266.

629 Szabo TM, McCormick CA, Faber DS (2007) Otolith endorgan input to the Mauthner neuron in the
630 goldfish. J Comp Neurol 505:511–525.

Szabo TM, Weiss SA, Faber DS, Preuss T (2006) Representation of auditory signals in the M-cell: role of electrical synapses. J Neurophysiol 95:2617–2629.

Tabor KM, Smith TS, Brown M, Bergeron SA, Briggman KL, Burgess HA (2018) Presynaptic Inhibition Selectively Gates Auditory Transmission to the Brainstem Startle Circuit. Curr Biol CB 28:2527-2535.e8.

Temizer I, Donovan JC, Baier H, Semmelhack JL (2015) A Visual Pathway for Looming-Evoked Escape in Larval Zebrafish. Curr Biol CB 25:1823–1834.

Wallace MT, Meredith MA, Stein BE (1998) Multisensory integration in the superior colliculus of the alert cat. J Neurophysiol 80:1006–1010.

Wei P, Liu N, Zhang Z, Liu X, Tang Y, He X, Wu B, Zhou Z, Liu Y, Li J, Zhang Y, Zhou X, Xu L, Chen L, Bi G, Hu X, Xu F, Wang L (2015) Processing of visually evoked innate fear by a non-canonical thalamic pathway. Nat Commun 6:6756.

Weiss SA, Preuss T, Faber DS (2009) Phase encoding in the Mauthner system: implications in left-right sound source discrimination. J Neurosci 29:3431–3441.

Weiss SA, Zottoli SJ, Do SC, Faber DS, Preuss T (2006) Correlation of C-start behaviors with neural activity recorded from the hindbrain in free-swimming goldfish (Carassius auratus). J Exp Biol 209:4788–4801.

Zheng A, Schmid S (2023) A review of the neural basis underlying the acoustic startle response with a focus on recent developments in mammals. Neurosci Biobehav Rev 148:105129.

Zhou G, Lane G, Noto T, Arabkheradmand G, Gottfried JA, Schuele SU, Rosenow JM, Olofsson JK, Wilson DA, Zelano C (2019) Human olfactory-auditory integration requires phase synchrony between sensory cortices. Nat Commun 10:1168.

Zottoli SJ (1977) Correlation of the startle reflex and Mauthner cell auditory responses in unrestrained goldfish. J Exp Biol 66:243–254.

Zottoli SJ, Hordes AR, Faber DS (1987) Localization of optic tectal input to the ventral dendrite of the goldfish Mauthner cell. Brain Res 401:113–121.

Zwaka H, McGinnis OJ, Pflitsch P, Prabha S, Mansinghka V, Engert F, Bolton AD (2022) Visual object detection biases escape trajectories following acoustic startle in larval zebrafish. Curr Biol 32:5116-5125.e3.

661 FIGURE LEGENDS

662 **Figure 1**. M-cell responses to tectal stimulation. A. M-cell responses to a 60 Hz tectal train of 200 ms
663 were used to measure the evoked depolarization at 1, 33, 100 and 200 ms after stimulus onset during
664 a 12-ms time window (colored vertical boxes). A´. Blue and orange bars in the trace show the tonic
665 and phasic components of the response, respectively. The horizontal dotted lines indicate the baseline
666 (bottom) and the potential before the last pulse for quantification of each component. B. Mean
667 amplitude (± SEM) of the phasic (shades of orange) and tonic (shades of blue) components of tectal
668 trains for the time windows described in A. C. M-cell responses to a 100 ms tectal pulse train of 30,
669 60, 100 or 200 Hz were recorded and quantified as in A, at the end of the pulse. D. Mean amplitude (±
670 SEM) of the phasic (shades of orange) and tonic (shades of blue) components of 100-ms tectal trains
671 of different frequency.

672

673 **Figure 2**. Multisensory integration in the M-cell. A. Diagram of stimulation (left) and response
674 examples (right). The response examples correspond, to a single acoustic pulse (blue trace) and to
675 their multisensory combination (purple). Below the traces diagram of the stimulation is shown in gray.
676 B. Stacked bars comparing mean (± SEM) depolarization evoked by tectal trains of indicated duration
677 (T, orange), auditory (A, blue) or their multisensory combination (purple). C. Boxplots showing the
678 ratios between the multisensory responses and the maximum unisensory response (MSI/Max). D.
679 Boxplots showing the ratios between the multisensory responses and the sum of its unisensory
680 components (MSI/Sum). E-H. As in A-D but for 100 ms tectal trains of different frequencies.

681

682 **Figure 3**. Auditory and tectal FFI have different decay dynamics. A. Diagram of auditory or tectal
683 feedforward inhibition circuits (center), and the quantification of sensory evoked shunting inhibition
684 as a reduction of M-cell AP amplitude (left, auditory: shaded-blue area; right, tectal: shaded-red area)
685 to a control AP (black trace). B-C. Boxplots of peak inhibition and time of peak inhibition triggered by
686 acoustic or tectal stimuli. D. Mean (±SEM) FFI triggered by tectal and auditory inputs measured in the
687 same M-cells at different time points between 0 and 70 ms post-stimulus. E. Boxplot of the time
688 elapsed to 50% decay of peak FFI for the auditory (left) and tectal (right) stimuli. *p=0.0145. F. Area
689 below the curve (0-70 ms) for the auditory (left) and tectal (right) stimuli. *p=0.0181.

690

691 **Figure 4**. Effect of stimulus sequence and modality on M-cell integration. A. Representative responses
692 of one M-cell to two stimuli presented in different trials, or in the same trials with a 50 ms offset. The
693 upper trace shows the M-cell response to an auditory stimulus (S1/A), middle trace corresponds to
694 the response to a single tectal pulse (S2/T) and bottom trace shows the response to an A stimulus
695 followed by a T stimulus 50 ms later. The area used to quantify each response is shaded in orange
696 (Resp1), dark green (Resp2) or light green (Resp(1+2)) respectively. Schematics below each trace the
697 order of stimuli and the area where responses were quantified. The pink bar indicates the time point
698 at which the lingering depolarization of the first response was measured. Note that this analysis was
699 performed for trials in which S1 and S2 could be either A or T, resulting in trials AA, TT, TA and AT
700 sequences. B. Lingering depolarization after 50 ms of a single auditory pip or a short tectal train.
701 *p=0.0188. C. Integration in the M-cell for pairs of uni- or multisensory stimuli with a 50 ms delay was
702 calculated as the ratio: Resp (1+2) / (Resp1 + Resp2).

703

704 **Figure 5**. Multisensory integration of subthreshold unisensory stimuli. A. MSI/Max vs. the maximum
705 unisensory response of different multisensory stimuli, irrespective of duration, frequency, or
706 sequence of stimulation. B. Similar to A, but with the MSI/Sum instead vs. the sum of the unisensory
707 responses. C. Example traces in which the integration of subthreshold unisensory tectal (T, red) and
708 auditory (A, blue) stimuli evokes an M-cell AP (TA, purple). Responses to an auditory pip only triggered
709 an action potential when they were preceded by four tectal pulses delivered at 333Hz (left) or a 200-
710 ms tectal train at 60Hz (right).

711

712 **Supplementary Figure 1**. A-B. Representative recordings of left or right M-cell somatic responses to
713 an electric stimulus train delivered to the left tectum (A) or to a short 200 Hz sound pip produced by
714 a loudspeaker placed to the right side of the fish (B). The mean (of 3-5 repetitions) response is shown
715 in solid color and the diagram of the tectal stimulus or the sound pip are shown below the traces.
716 Dashed boxes indicate the 12-ms time windows following the stimulus where the responses were
717 quantified. C-D. Boxplots showing the median, upper and lower quartiles and comparing the response
718 to the same stimulus in the left or right M-cell in 9 fish for the tectal stimulus (C) and 11 fish for the
719 auditory stimulus (D). Markers with the same color in left and right belong to pairs of M-cells of the
720 same fish. No differences were found in the evoked response amplitude between the left and right M-
721 cells or for tectal or auditory stimuli.

# Figure 1

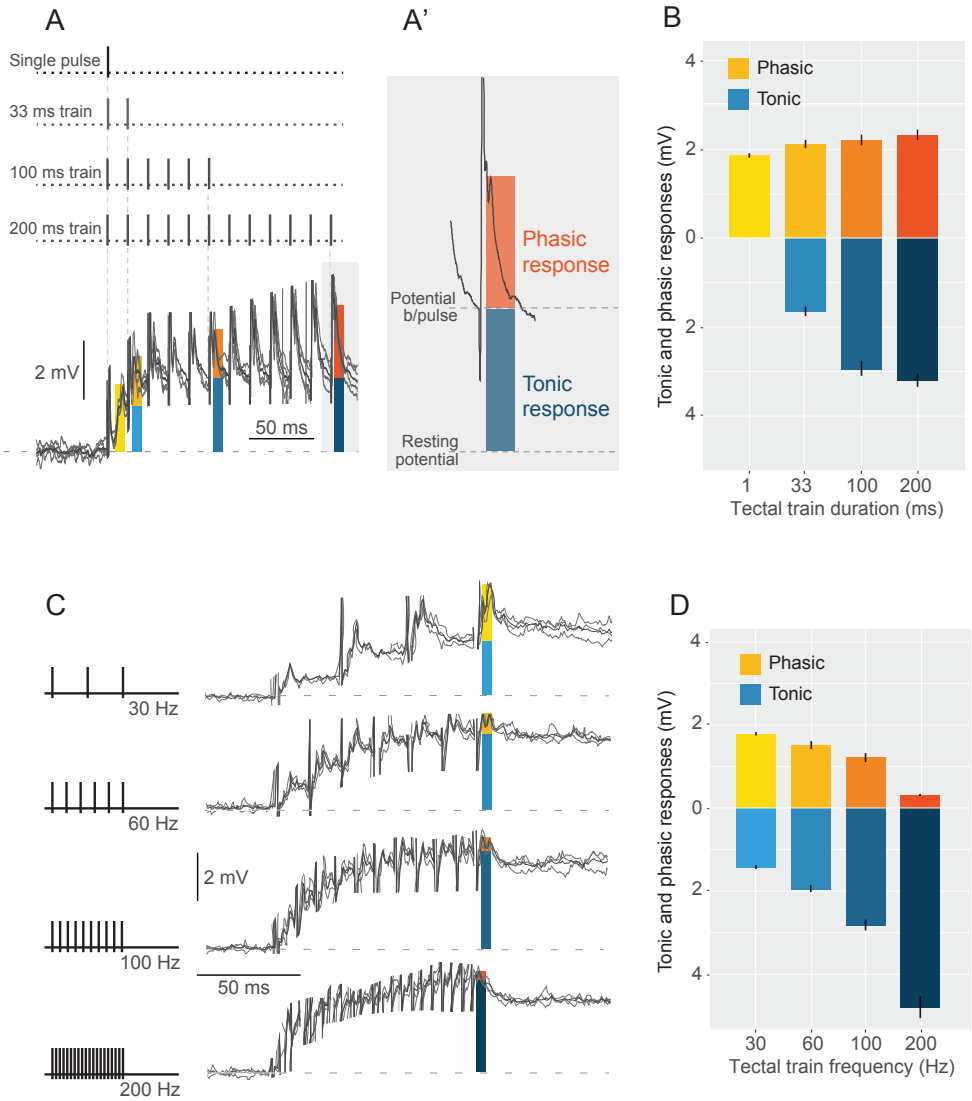


**Figure 1. M-cell responses to tectal stimulation**. A. M-cell responses to a 60 Hz tectal train of 200 ms were used to measure the evoked depolarization at 1, 33, 100 and 200 ms after stimulus onset during a 12-ms time window (colored vertical boxes). A´. Blue and orange bars in the trace show the tonic and phasic components of the response, respectively. The horizontal dotted lines indicate the baseline (bottom) and the potential before the last pulse for quantification of each component. B. Mean amplitude (± SEM) of the phasic (shades of orange) and tonic (shades of blue) components of tectal trains for the time windows described in A. C. M-cell responses to a 100 ms tectal pulse train of 30, 60, 100 or 200 Hz were recorded and quantified as in A, at the end of the pulse. D. Mean amplitude (± SEM) of the phasic (shades of orange) and tonic (shades of blue) components of 100-ms tectal trains of different frequency.

# Figure 2

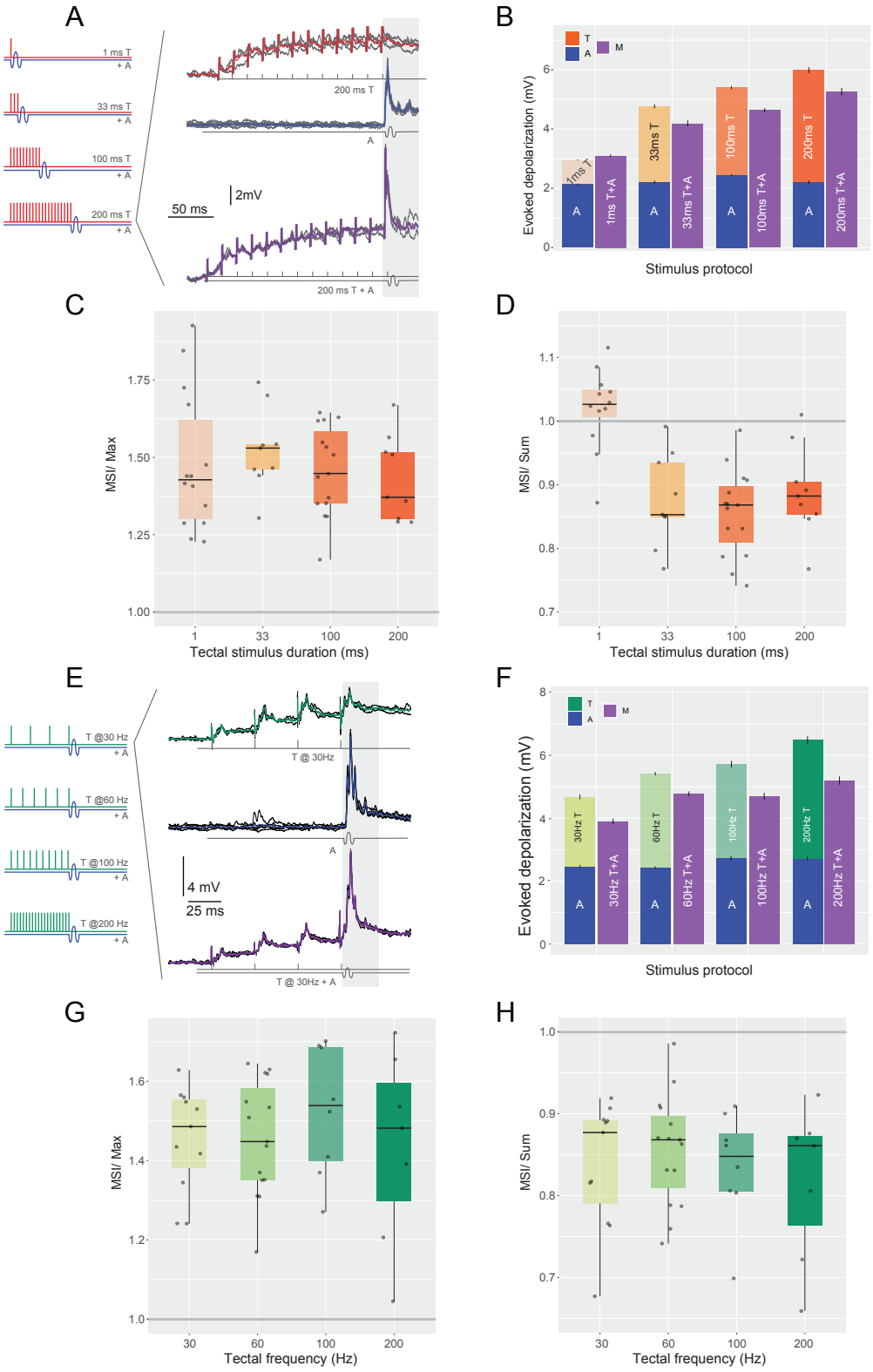


**Figure 2. Multisensory integration in the M-cell.** A. Diagram of stimulation (left) and response examples (right). The response examples correspond, to a single acoustic pulse (blue trace) and to their multisensory combination (purple). Below the traces diagram of the stimulation is shown in gray. B. Stacked bars comparing mean (± SEM) depolarization evoked by tectal trains of indicated duration (T, orange), auditory (A, blue) or their multisensory combination (purple). C. Boxplots showing the ratios between the multisensory responses and the maximum unisensory response (MSI/Max). D. Boxplots showing the ratios between the multisensory responses and the sum of its unisensory components (MSI/Sum). E-H. As in A-D but for 100 ms tectal trains of different frequencies.

Figure 3

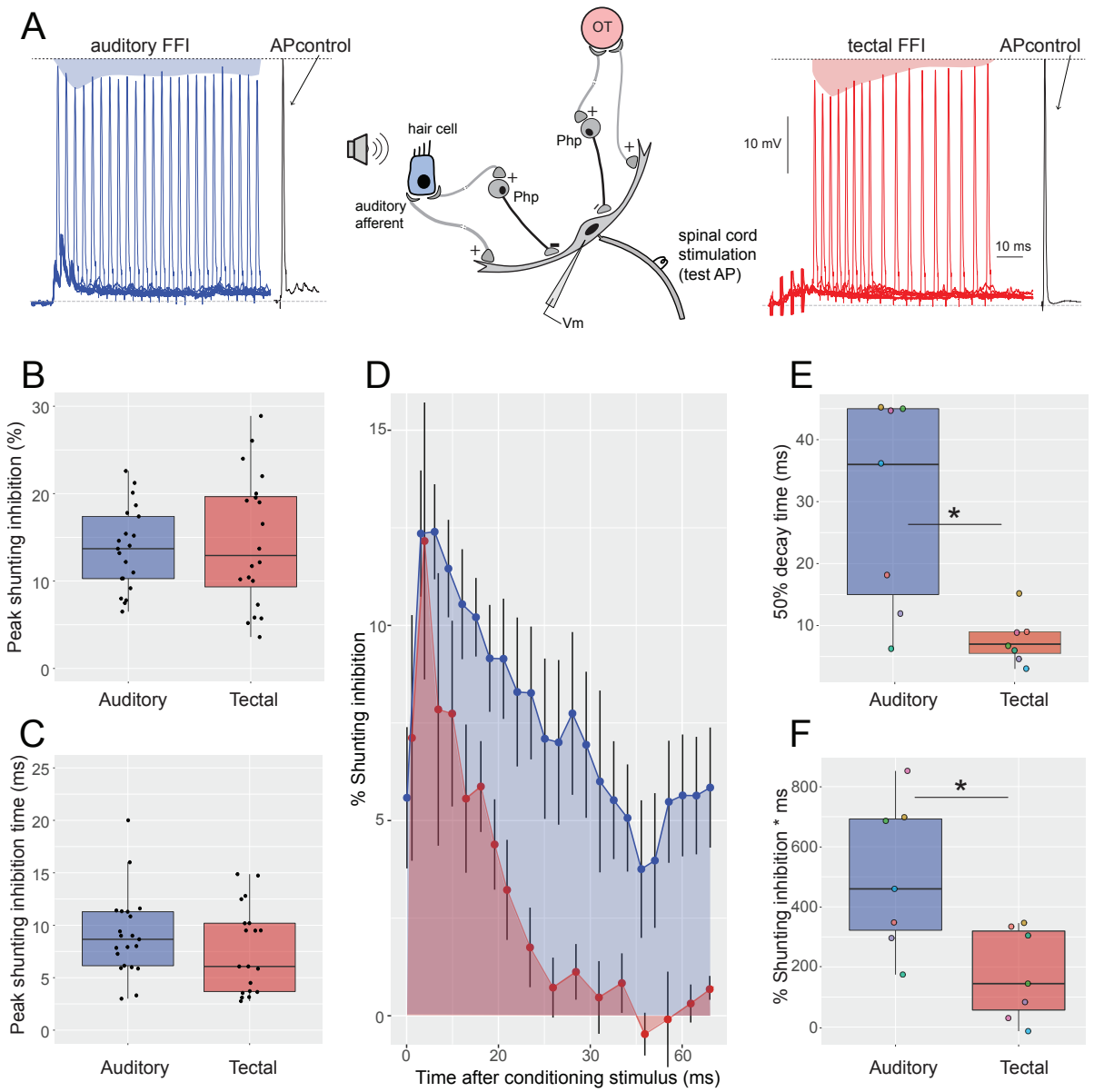


**Figure 3. Auditory and tectal FFI have different decay dynamics.** A. Diagram of auditory or tectal feedforward inhibition circuits (center), and the quantification of sensory evoked shunting inhibition as a reduction of M-cell AP amplitude (left, auditory: shaded-blue area; right, tectal: shaded-red area) to a control AP (black trace). B-C. Boxplots of peak inhibition and time of peak inhibition triggered by acoustic or tectal stimuli. D. Mean (±SEM) FFI triggered by tectal and auditory inputs measured in the same M-cells at different time points between 0 and 70 ms post-stimulus. E. Boxplot of the time elapsed to 50% decay of peak FFI for the auditory (left) and tectal (right) stimuli. *p=0.0145. F. Area below the curve (0-70 ms) for the auditory (left) and tectal (right) stimuli. *p=0.0181.

Figure 4

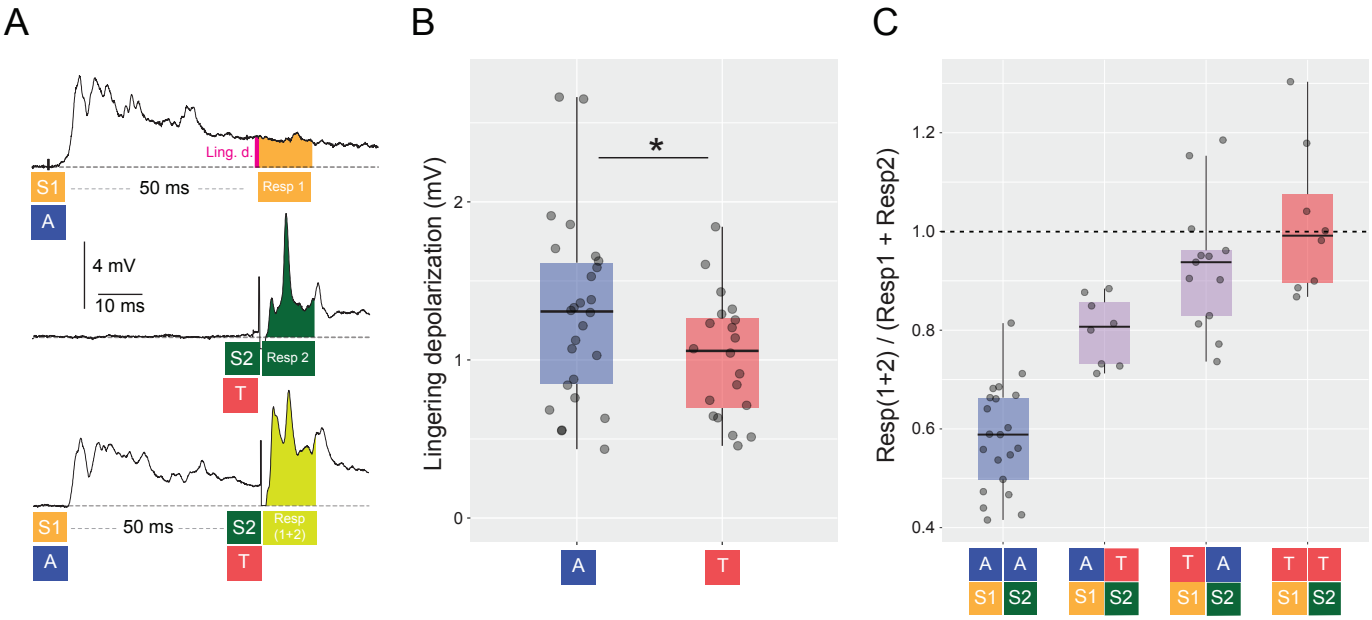


**Figure 4. Effect of stimulus sequence and modality on M-cell integration.** A. Representative responses of one M-cell to two stimuli presented in different trials, or in the same trials with a 50 ms offset. The upper trace shows the M-cell response to an auditory stimulus (S1/A), middle trace corresponds to the response to a single tectal pulse (S2/T) and bottom trace shows the response to an A stimulus followed by a T stimulus 50 ms later. The area used to quantify each response is shaded in orange (Resp1), dark green (Resp2) or light green (Resp(1+2)) respectively. Schematics below each trace the order of stimuli and the area where responses were quantified. The pink bar indicates the time point at which the lingering depolarization of the first response was measured. Note that this analysis was performed for trials in which S1 and S2 could be either A or T, resulting in trials AA, TT, TA and AT sequences. B. Lingering depolarization after 50 ms of a single auditory pip or a short tectal train. *p=0.0188. C. Integration in the M-cell for pairs of uni- or multisensory stimuli with a 50 ms delay was calculated as the ratio: Resp (1+2) / (Resp1 + Resp2).

Figure 5

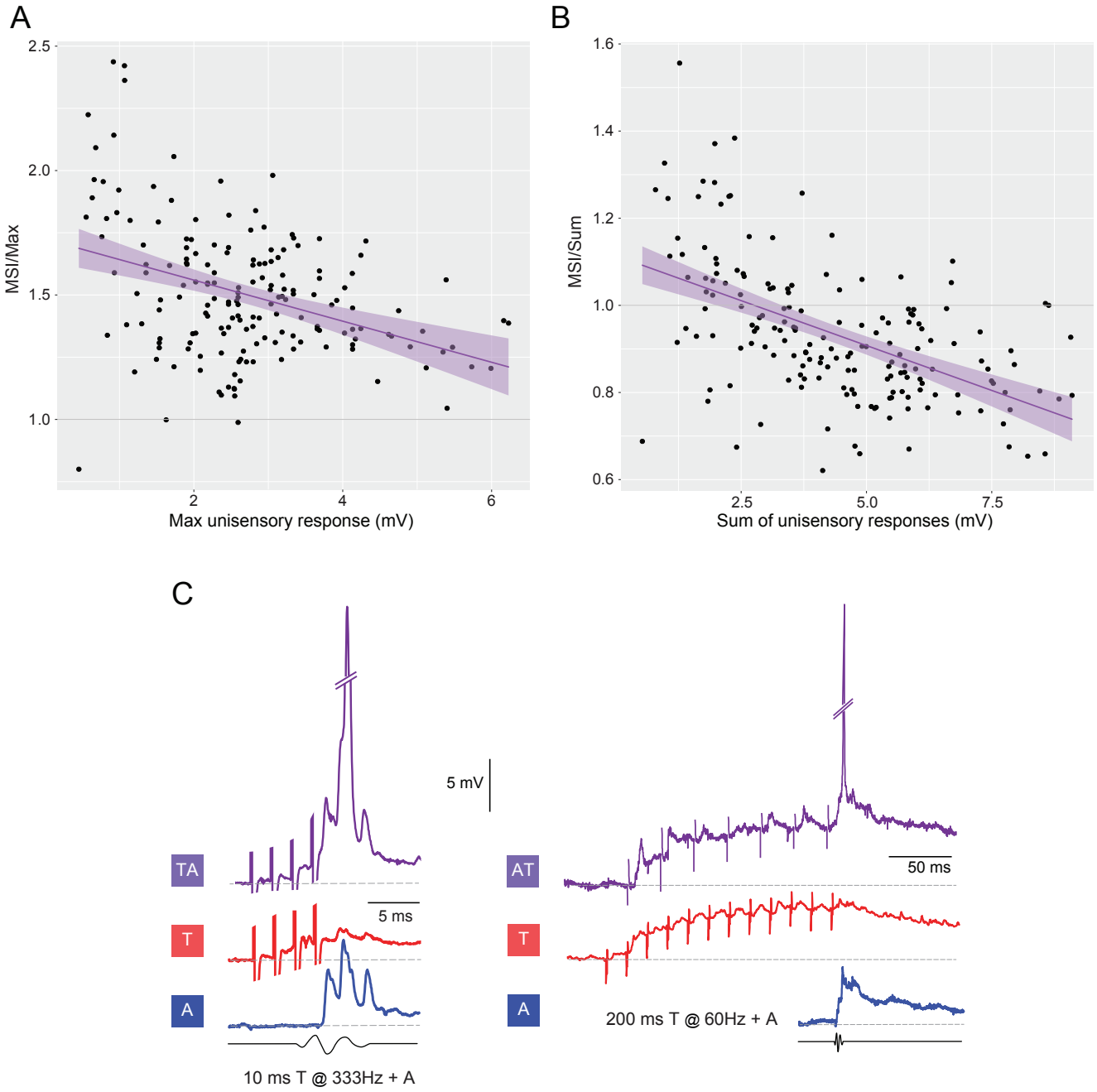


**Figure 5. Multisensory integration of subthreshold unisensory stimuli.** A. MSI/Max vs. the maximum unisensory response of different multisensory stimuli, irrespective of duration, frequency, or sequence of stimulation. B. Similar to A, but with the MSI/Sum instead vs. the sum of the unisensory responses. C. Example traces in which the integration of subthreshold unisensory tectal (T, red) and auditory (A, blue) stimuli evokes an M-cell AP (TA, purple). Responses to an auditory pip only triggered an action potential when they were preceded by four tectal pulses delivered at 333Hz (left) or a 200-ms tectal train at 60Hz (right).

# Supplementary Figure 1

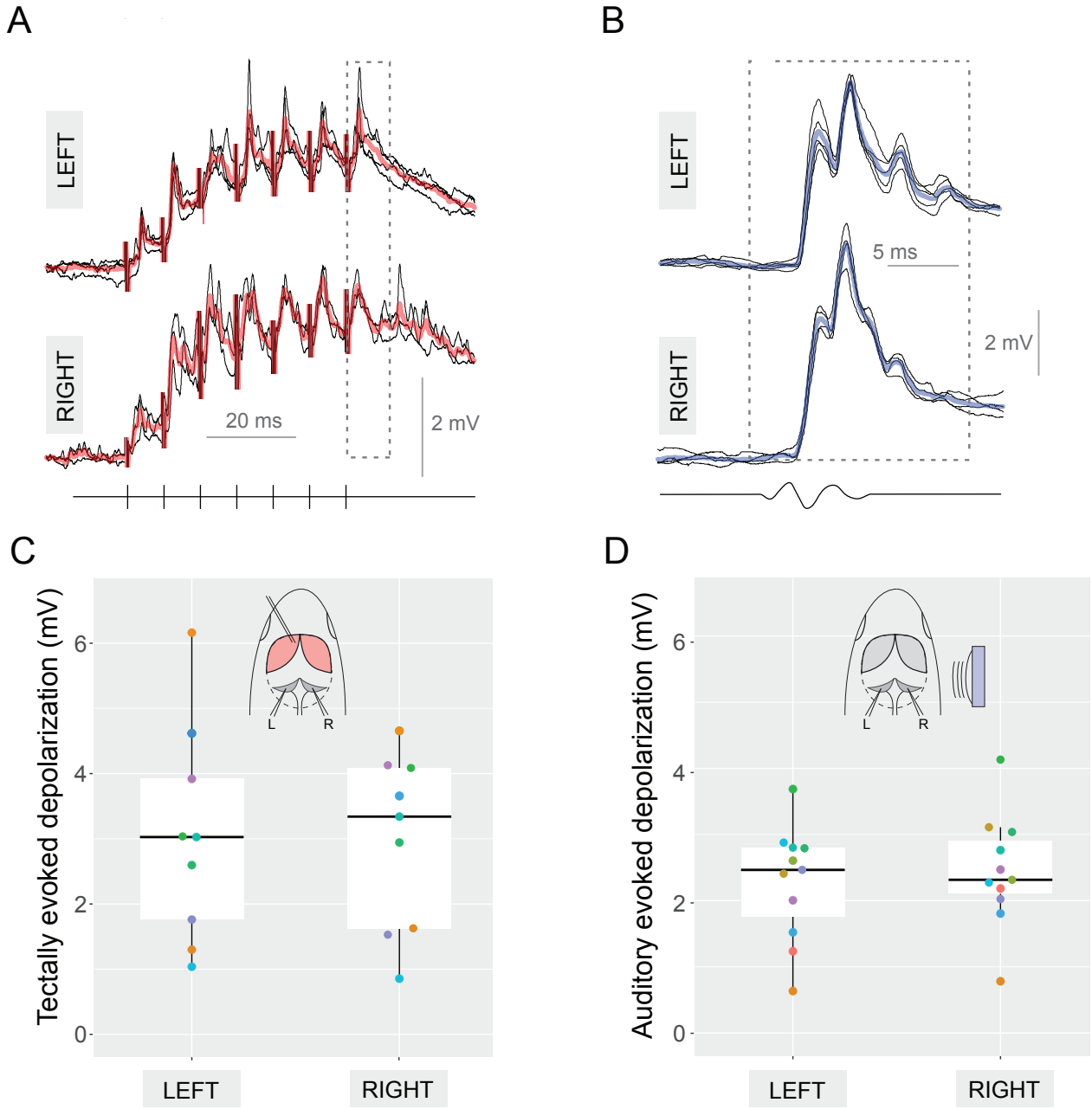


**Supplementary Figure 1. A-B.** Representative recordings of left or right M-cell somatic responses to an electric stimulus train delivered to the left tectum (A) or to a short 200 Hz sound pip produced by a loudspeaker placed to the right side of the fish (B). The mean (of 3-5 repetitions) response is shown in solid color and the diagram of the tectal stimulus or the sound pip are shown below the traces. Dashed boxes indicate the 12-ms time windows following the stimulus where the responses were quantified. C-D. Boxplots showing the median, upper and lower quartiles and comparing the response to the same stimulus in the left or right M-cell in 9 fish for the tectal stimulus (C) and 11 fish for the auditory stimulus (D). Markers with the same color in left and right belong to pairs of M-cells of the same fish. No differences were found in the evoked response amplitude between the left and right M-cells or for tectal or auditory stimuli.